Journal of Applied Polymer Science

Effects of substitution for carbon black with graphene oxide or graphene on the morphology and performance of natural rubber/carbon black composites

Ganwei Yang, Zhenfei Liao, Zhijun Yang, Zhenghai Tang, Baochun Guo
Department of Polymer Materials and Engineering, South China University of Technology, Guangzhou 510640, China
Correspondence to: B. Guo (E-mail: psbcguo@scut.edu.cn)

ABSTRACT: In this study, nanosheets including graphene oxide (GO) and reduced graphene oxide (rGO), were incorporated into natural rubber (NR), to study the effects of substituting GO or rGO for carbon black (CB) on the structure and performance of NR/CB composites. The morphological observations revealed the dispersion of CB was improved by partially substituting nanosheets for CB. The improvements in static and dynamic mechanical properties were achieved at small substitution content of GO or rGO nanosheets. With substitution of rGO nanosheets, significant improvement in flex cracking resistance was achieved. NR/CB/rGO (NRG) composites has a much lower heat build-up value compared with NR/CB/GO (NG) composites at a high load of nanosheets. However, both GO and rGO tended to aggregate at a high concentration, which led to the poor efficiency on enhancing the dynamic properties, or even deteriorate the performance of rubber composites. © 2015 Wiley Periodicals, Inc. J. Appl. Polym. Sci. **2015**, *132*, 41832.

KEYWORDS: composites; graphene and fullerenes; mechanical properties; nanotubes; rubber

Received 25 September 2014; accepted 6 December 2014
DOI: 10.1002/app.41832

INTRODUCTION

Graphene, which is under the spotlight of scientific and technological circles in recent years, has been incorporated in various polymer matrices to prepare the nanocomposites for taking advantage of its excellent properties. However, it is still a challenge to disperse graphene homogeneously and stably in polymer matrix, which is impeding the practical application of graphene in polymer composites.[1,2] Therefore, the modification of graphene has been accepted as a valid route for its application in polymers. Graphene oxide (GO), a derivative of graphene, is prepared by controllable oxidation of graphite by which abundant oxygen-containing groups are introduced into the graphene layers.[3–5] With abundant hydrophilic groups, GO is water-soluble so stable colloidal suspensions is easily achieved.[6] Due to the excellent stability of GO aqueous suspension, compounding GO suspension with rubber latices is convenient for fabricating rubber/GO composites. However, Li *et al.* reported that graphene performs more effectively in reinforcing natural rubber compared with GO, because graphene can give rise to a faster stain-induced crystallization rate and a higher crystallinity in NR.[7] In this study, we used tea polyphenols (TPs) as the reductants for GO to prepare TPs-reduced GO (rGO). Simultaneously, TPs served as the stabilizer for rGO.[8] In addition, as a natural antioxidant, the residue TPs on rGO are supposed to be helpful in enhancing the dynamic properties of rubber composites, on account of its reaction with the reactive oxygen species generated under dynamic environment.[9]

Numerous inorganics or carbonaceous fillers have been utilized to reinforce rubber such as carbon black (CB), silica, clays, boehmite, carbon nanotubes (CNTs), etc.[10–14] However, single filler is not usually able to meet the comprehensive performance requirement of rubber products. Using the hybrid fillers, which contain two or even more kinds of fillers for rubber reinfocrement, has been a common practice in both academic and industrial communities. For example, Cabots developed dual phase filler by hybridizing CB with silica, which significantly improved the dynamic properties of rubber.[15] In recent years, numerous hybrid fillers system such as nanoclay/CB,[16] CNTs/CB,[17] CNTs/nanoclay,[18] and tubular clay/graphene[19] have been introduced into rubbers for better reinforcements. It has been demonstrated that by combining the advantages of different kinds of fillers, synergistic enhancements on the properties of polymer composites were achieved in some cases. As the commonly used reinforcement filler, CB has been widely used in rubber industries especially tire industry. The investigation on the effects of hybridization of CB with other nanoparticle for rubber reinforcement is of great importance. Qu *et al.* reported a synergistic effect between CB and nanoclay in reinforcing rubber composites, giving rise to 147% increase on the tensile

Table I. Compositions of NG and NRG Nanocomposites

Samples[a]	NG-0	NG-0.5	NG-1	NG-3	NG-5	NRG-0.5	NRG-1	NRG-3	NRG-5
NR(dry)	100	100	100	100	100	100	100	100	100
GO	0	0.5	1	3	5	-	-	-	-
rGO	0	-	-	-	-	0.5	1	3	5
N330	40	39.5	39	37	35	39.5	39	37	35

[a] All the samples contain the below additives. Zinc oxide (5), stearic acid (2), *N*-isopropyl-*N*′-phenyl-p-phenylenediamine (1), 2,2′-dibenzothiazoledisulfde (0.5), *N*-cyclohexylbenzothiazole-2-sulphenamide (0.5) and sulfur (2).

strength.[16] It's been investigated by Zhang *et al.* that, by replacing partial CB with multi-walled carbon nanotubes (MWNTs), the percolation threshold of conductive polymer composites(CPCs) was much lower than that of CPCs filled with MWNTs or CB only.[20] A synergistic effect was confirmed by adding carbon nanotubes (CNTs) to the CB-filled *trans*-polyisoprene (TPI), which led to significant synergy in modulus.[21] To the best of our knowledge, utilizing CB/modified graphene hybrid filler for rubber reinforcement has not been reported.

In this study, two hybrid fillers systems, GO/CB and rGO/CB hybrid fillers systems, were developed. With keeping the total mass fraction of fillers as a constant, we studied the effects of substituting GO or rGO nanosheets for CB on the structure and performance of NR/CB composites. In the meanwhile, morphology and properties of NR/GO/CB (NG) and NR/rGO/CB (NRG) composites were investigated, and their static and dynamic mechanical properties were systematically evaluated.

EXPERIMENTAL

Materials

Graphite powder (<20 μm) was purchased from Shanghai Colloidal. The reagents used for the oxidation of graphite, including concentrated sulfuric acid (H_2SO_4), hydrochloric acid (HCl), potassium permanganate ($KMnO_4$), and sodium nitrate ($NaNO_3$), and 30 wt % of hydrogen peroxide (H_2O_2) were analytically pure and used as received. TPs (purity of 98%) were purchased from Xi'an Haoxuan Biotechnology Limited, Xi'an, China. Natural rubber latex (NR, 60 wt %) was provided by Chinese Academy of Tropical Agriculture Sciences. Carbon black (CB, N330) was provided by Shanghai Cabot Chemical. The other rubber compound ingredients were all commercially available and used as received.

Preparation of GO and rGO

GO was synthesized by oxidation of purified natural graphite powder by a modified Hummers method.[3] rGO was reduced and modified by tea polyphenols(TPs), which was employed as a reducer and stabilizer.[8] Typically, TPs (300 wt % relative to GO) were added into the as-prepared GO aqueous solution (1 mg mL^{-1}), and then after sonication for 30 min, the mixture was maintained at 80°C for 8 h under stirring. Then the residue TPs on the rGO were removed by repeated washed with plenty of deionized water and centrifugation.

Preparation of Rubber Composites

Quantitative GO was dispersed into deionized water by ultrasonication to prepare 1 mg mL^{-1} GO colloidal dispersion, then added into NR latex and stirred for 1 h. So did the as-prepared rGO colloidal dispersion. Calcium chloride solution (1 mg mL^{-1}) was used to coagulate NR/GO and NR/rGO compounds. The coagulated compounds were washed for several times to remove the remnant flocculants, and then vacuum dried at 50°C overnight.

The samples of rubber composites are referred to as NG-x or NRG-x for the NR/CB/GO or NR/CB/rGO systems, respectively, and x corresponds to the mass fraction of GO or rGO that is substituted for CB. The formulations of the NG and NRG composites are list in Table I. The compounds were hot-pressed and vulcanized at 143°C × Tc_{90} under the pressure of 15 MPa. Tc_{90} was measured by an UR2030 rheometer (U-CAN DYNATEX, Taiwan, China).

Characterization

Processability of rubber compounds was tested on Rubber Process Analyzer (RPA 2000, Alpha Technology, USA). The compounds were scanned in a strain scanning mode from 0.28% to 350%, while temperature and frequency were fixed at 60°C and 1 Hz, respectively. The cryogenically fractured surfaces of the rubber composites were observed by a field emission scanning electron microscope (Hitachi S-4800, Japan). Before observation, the fracture surfaces were plated with a thin layer of gold. A JEM-2100(HR) Transmission Electron Microscope (TEM) made by JEOL in Japan was employed to examine the morphology of the composites. The TEM specimens were prepared by a Leica EM UC6 Ultracut Microtome and mounted on 200 mesh copper grids. Dynamic mechanical analysis (DMA) was carried out on an EPLEXOR dynamic mechanical analyzer (Gabo Qualimeter Testanlagen GmbH; Germany). The samples were scanned from −100 to 80°C in the tensile mode, with a heating rate of 3 K min^{-1} and a frequency of 5 Hz. Tensile tests were performed at 25°C, on an U-CAN UT-2060 (Taiwan) instrument, referring to ISO standard 37-2005. Shore A hardness was performed by an XY-1 sclerometer (Shanghai) according to ISO standard 7619-1997.

Equilibrium swelling method[22,23] was used to measure the crosslinking density of the vulcanizates. About 1 g of vulcanizate was weighed, noted as m_0, then swollen with toluene at room temperature for 72 h. After removing from the toluene and wiped off the surficial toluene, the samples were immediately weighed, noted as m_1, and then dried in a vacuum oven at 80°C for 36 h to remove all the solvent and reweighed, noted as m_2. The volume fraction of NR in the swollen gel (υ_r) was calculated by the following equation:

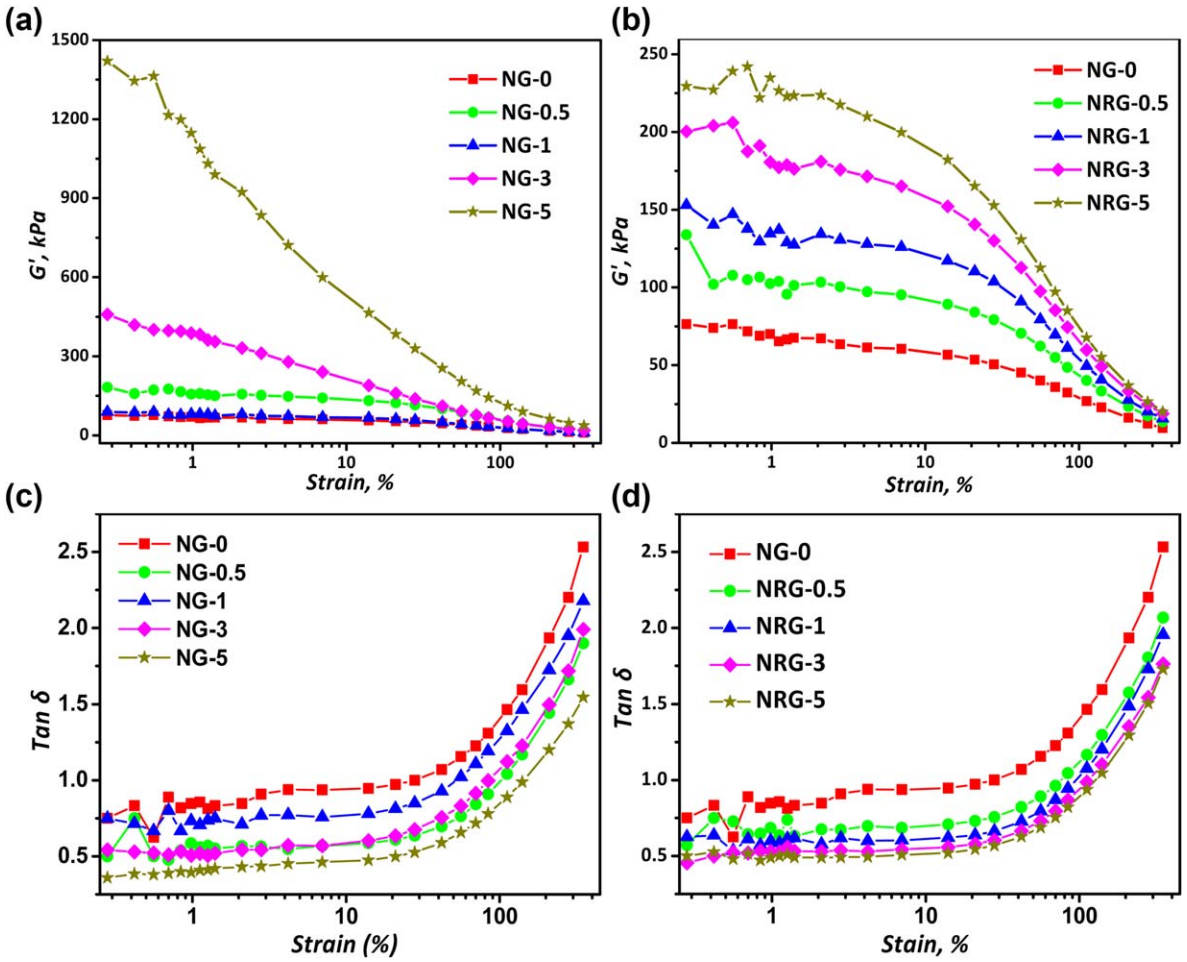

Figure 1. Dependences of storage modulus (a) and (b) and tan δ (c) and (d) on strain in NG and NRG compounds. [Color figure can be viewed in the online issue, which is available at wileyonlinelibrary.com.]

$$\upsilon_r = \frac{m_0 * \Phi * (1-\alpha)/\rho_r}{m_0 * \Phi * (1-\alpha)/\rho_r + (m_1 - m_2)/\rho_s} \quad (1)$$

where Φ is the mass fraction of rubber in the vulcanizates, α is the mass loss of NR vulcanizates during swelling, and ρ_r is density of rubber while ρ_s is the density of solvent.

The elastically active network chain density (υ_e) was used to represent the whole crosslink density, and it's calculated by the well-known Flory–Rehner equation:

$$\upsilon_e = -\frac{\ln(1-\upsilon_r) + \upsilon_r + \chi \upsilon_r^2}{\upsilon_s(\upsilon_r^{1/3} - \upsilon_r/2)} \quad (2)$$

where υ_r is the volume fraction of the polymer in the vulcanizate swollen to equilibrium and υ_s is the solvent molar volume (106.2 cm^3 mol^{-1} for toluene). χ is the interaction parameter between rubber and solvent (0.393 for the NR/toluene).[7]

Determination of flex cracking and crack growth (De Mattia) was performed on GT-7011-D flexing resistance tester (Gotech, Taiwan), according to GB/T 13934-2006 standard. Dynamic compression heat build-up test was performed on a U-Can UD-3801 dynamic compression heat build-up testing instrument, following GB/T 1687-1993 standard.

RESULTS AND DISCUSSION

Effects of the Substitution of GO or rGO on Filler Network

Dynamic strain sweeping was conducted to evaluate the filler network of rubber compounds, i.e., uncured rubber composites. The shear modulus of filler-reinforced rubber is strain dependent.[24] In the certain range, the shear modulus decreases rapidly as the strain increases. That is due to the collapsing of filler–filler network structure in rubber compounds, which is commonly known as Payne effect. In general, the filler network in rubber compounds is characterized by the difference of shear modulus ($\Delta G'$) between low strain (~0.5%) and higher strain (~100%).

Figure 1 shows the strain sweep of NR compounds at different nanosheets contents. It's obvious that the shear modulus of NR/CB compounds with GO or rGO significantly increase with the contents of GO or rGO [Figure 1(a,b)]. The modulus of the composite with GO is higher than that for the composite with rGO, especially at high content of substitution, such as 5 phr. However, the overlapped GO sheets are sensitive to strain, resulting in

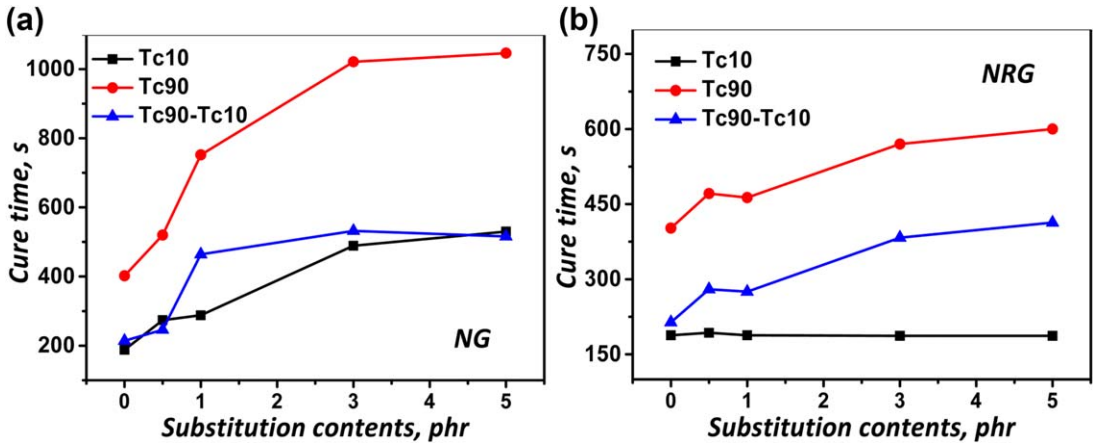

Figure 2. Effects of the substitution for CB with GO (a) or rGO (b) on the vulcanization characteristics of NR/CB composites. [Color figure can be viewed in the online issue, which is available at wileyonlinelibrary.com.]

abrupt collapsing of the GO network at small strain, suggesting weak interaction between CB and GO. In particular, the filler networks of NG-5 and NG-3 collapse at a small stain, which is likely due to more "trapped rubber" formed at higher GO content. However those "trapped rubber" are easily broken down in the uncured rubber compound under shearing because of the relatively poorer compatibility between GO and NR. So the degree of stability of filler networks is thought to be more important than the absolute value of G' to evaluate the developed degree of filler networks here. In comparison to CB/GO filled systems, the CB/rGO filled systems exhibit a stable platform due to stronger interaction between CB and rGO. Compared with the control sample (CB filled only), much apparent Payne effect is experienced in NG and NRG compounds, due to easier filler network of CB and the nanosheets with higher aspect ratio. Actually the dispersion of CB particles is improved due to the presence of the nanosheets which will be substantiated later.

From Figure 1(c,d), one can see that, with increasing nanosheets content, the tan δ of NG and NRG compounds decreases gradually. This implies that NG and NRG compounds would probably possess lower heat build-up during dynamic loading. This should be attributed to the improved dispersion of CB, which alleviates the destruction−aggregations of CB as well as the filler friction during dynamic service. This observation indicates the substituted composites may have promising application in dynamic environment such as tire tread. In addition, tan δ increases with the applied stain when it is higher than 10%. This could be due to two aspects.[25] For one thing, when the amplitude of stain increases to a level that can break up the filler networks, "trapped rubber" incorporated in the networks will be released to participate in the energy loss process and lead to the increase of tan δ. For another thing, under this condition, the destruction and regeneration of filler networks will also increase the energy loss of rubber composites. Both of these two processes enhance with an increasing amplitude of strain, so tan δ increases sharply as well.

Vulcanization Characteristics of NR/CB Composites

To interpret the effects of substituting GO or rGO for CB on the vulcanization, the curing parameters of NG and NRG composites are presented in Figure 2, and the data are summarized in Table II. Generally, Tc10 is used to evaluate the scorching safety and curing induction period, Tc90 is treated as the optimum curing time, and

Table II. Vulcanization Characteristics of NG and NRG Compounds

GO(rGO)/CB ratio	Ts1 (s)	Ts2 (s)	Tc10 (s)	Tc90 (s)	ML (dN m)	MH (dN m)
NG						
0/40	161	182	188	402	0.56	24.83
0.5/39.5	241	268	274	520	0.44	24.59
1/39	246	280	288	752	0.45	25.16
3/37	413	479	489	1021	0.56	23.00
5/35	439	522	530	1046	0.77	22.58
NRG						
0/40	161	182	188	402	0.56	24.83
0.5/39.5	179	196	193	471	0.20	17.58
1/39	175	189	188	463	0.27	19.01
3/37	168	185	187	570	0.62	22.73
5/35	168	190	187	600	0.47	19.06

the difference between Tc90 and Tc10 (Tc90–Tc10) is utilized to characterize the vulcanization rate. It is obvious that Tc10 and Tc90 of NG composites increase as GO loading, which suggests that addition of GO retards the curing. Because of the abundant functional groups on GO sheets, they tend to absorb the curing agents. It has been reported that accelerators tend to interact with GO to form hydrogen bonding due to their abundant surface functional groups, such as nitrogen atoms and sulfur atoms on the accelerators, and epoxy groups, carboxyl groups, hydroxyl groups on the GO sheets.[26] In addition, the retarded curing may also be due to the limited diffusion of curing agents by formation of hybrid fillers network.[27] Consequently, with more GO substituted for CB, the curing process of NG composites is more retarded. In the contrast, rGO seems to have no detrimental effects on curing introduction period. Substituting rGO for CB also delays the curing progress, which may also be attributed to the restricted diffusion and the adsorption of curatives on the surface of rGO. However, due to different surface chemistry, the functional groups such as quinonyl groups[8] may reactive to sulfide radical, resulting faster curing in the composites with rGO.

Regarding the ML for NG and NRG, the ML is decreased when the content of GO or rGO is low, implying that the CB agglomerates are separated by the incorporated sheets (as will be discussed below). The incorporation of excessive nanosheets will lead to the self-aggregation of the nanosheets, and therefore resulting in an increased ML. From Table II, it can be seen that there is no distinct trend for MH with filler loading. This may be because the MH of the composites is influenced by multifactors such as filler dispersion and crosslink density.

Crosslink Density of NG and NRG Composites with Different Nanosheets Contents

Figure 3 depicts crosslink density of NG and NRG composites with changing content of GO and rGO. The crosslink density of the composites initially increases with the increasing nanosheets content, and subsequently starts to decrease at a certain content of nanosheets. NG composite achieves the maximum with addition of 1 phr of GO while NRG composite has the maximum crosslink density at rGO content of 3 phr. Such parabolic variation trend of crosslink density for both NG and NRG composites, could be accounted for two opposite effects. On one hand, GO and rGO sheets having high aspect ratio may serve additional physic crosslinks for rubber. In addition, it's been reported that the galloyl-derived orthquinone can be easily captured by thiol-based nucleophiles.[8,28] As a result, the galloyl-derived orthquinone of oxidized-TPs absorbed on rGO is likely to react with thiol groups generated during vulcanization in the case of sulfur-curing system, which can improve the crosslink density through covalent linkage between rGO and NR. On the other hand, GO or rGO tend to absorb accelerators as mentioned above, which delays the vulcanization and decreases crosslink density. Consequently the addition of GO or rGO sheets delay the vulcanization in different degrees. So it's rational to conclude that the variation of crosslink density is interpreted as the competitive result of two opposite effects induced by GO and rGO.

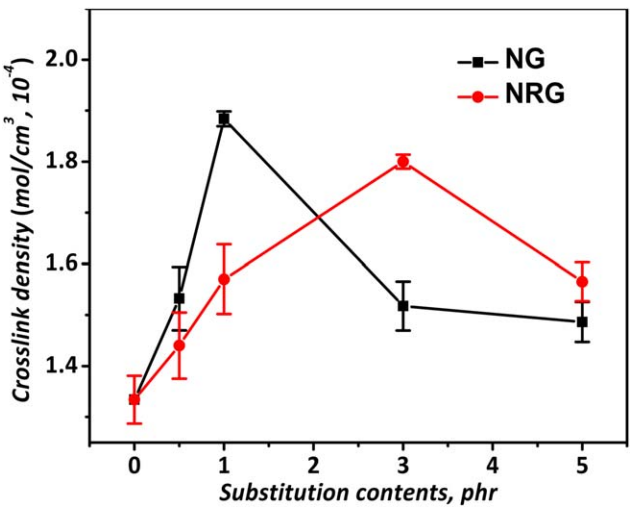

Figure 3. Effects of the substitution on the crosslink density of NR/CB composites. [Color figure can be viewed in the online issue, which is available at wileyonlinelibrary.com.]

Effects of the Substitution of GO or rGO on the Morphology of NR/CB Composites

SEM was utilized to study the morphology and evaluate the interfacial interactions in NG and NRG composites. Some representative images of the cryo-fractured surfaces of NG and NRG composites are shown in Figure 4. These sheet-like protuberances (indicated by red circles) on the fractured surface of composites with hybrid fillers, which is attributed to the embedding of nanosheets in the NR matrix, may provide indication interfacial interaction between the nanosheets and the matrix. It is obvious that the sheet-liked protuberances of NRG composites are rougher than that in NG composites, indicating a better compatibility of rGO with NR compared with GO. This should be attributed to the improved affinity between rGO and the matrix, which is realized through the possible interfacial crosslinking between the galloyl-derived orthquinone on rGO and the thiols generated during the vulcanization.[8,28] However, GO sheets, containing abundant surface oxygenic groups, exhibit low compatibility with the nonpolar NR chains resulted in the lower interfacial bonding results. Furthermore, some apparent aggregations of nanosheets were observed at 3 phr substitution content cases in both NG and NRG composites, whose thicknesses are several times of those at 1 phr substitution content case. The aggregations of nanosheets were thought to be the reason for inefficiency of nanosheets at a relatively higher concentration. In addition, it can be observed that the CB particles are dispersed more uniformly in NRG composites than those in NG composites, which reveals that rGO may play a positive role in promoting the dispersion of CB. It will be evidenced further by TEM.

TEM was employed to characterize the dispersion state of the nanosheet-substituted composites (Figure 5). Overall, the substituted composites exhibit uniform dispersion of the fillers, in which the nanosheets are dispersed among the CB particles. Compared with the composites filled with CB only, the dispersion of CB in nanosheet-substituted composites is improved, and the aggregates of CB become smaller. Furthermore, compared with NG composites, a more developed filler network can be observed in NRG composites, which is consistent with the results of RPA that rGO tends to promote a more stable filler networks.

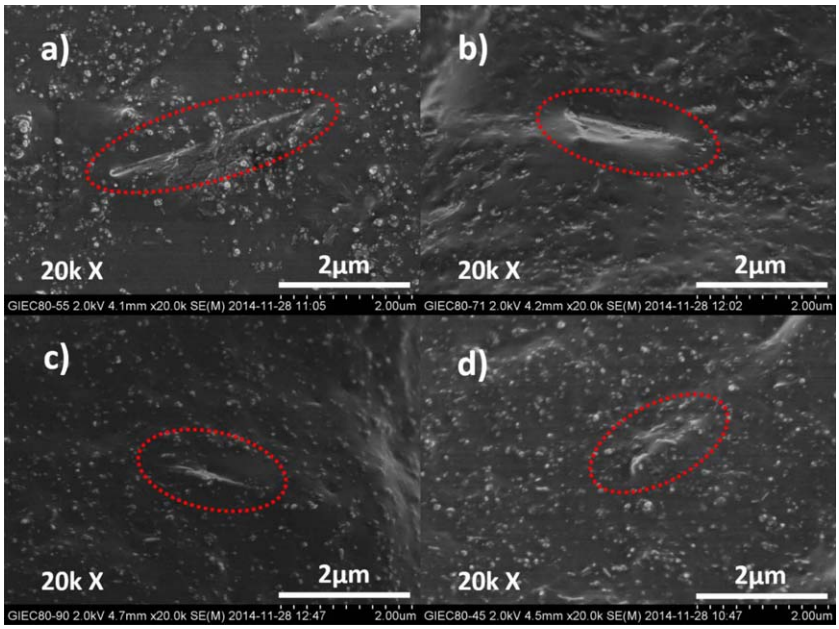

Figure 4. Effects of substitution on the morphology of the fractured surface of the composites evidenced by SEM. (a) NG-1; (b) NG-3; (c) NRG-1; (d) NRG-3. [Color figure can be viewed in the online issue, which is available at wileyonlinelibrary.com.]

It's noticeable that, at relatively high nanosheet loading (5 phr), both GO and rGO sheets [Figure 5(e,f)] are not fully exfoliated in the composites, which is attribute to the inevitable aggregation due to the interlayer Van der Waals forces and hydrogen bonding of nanosheets. The aggregation of GO sheets is found to be more serious than rGO at the same concentration. This observation further demonstrates that GO shows weaker interaction with NR matrix compared with rGO. The improved

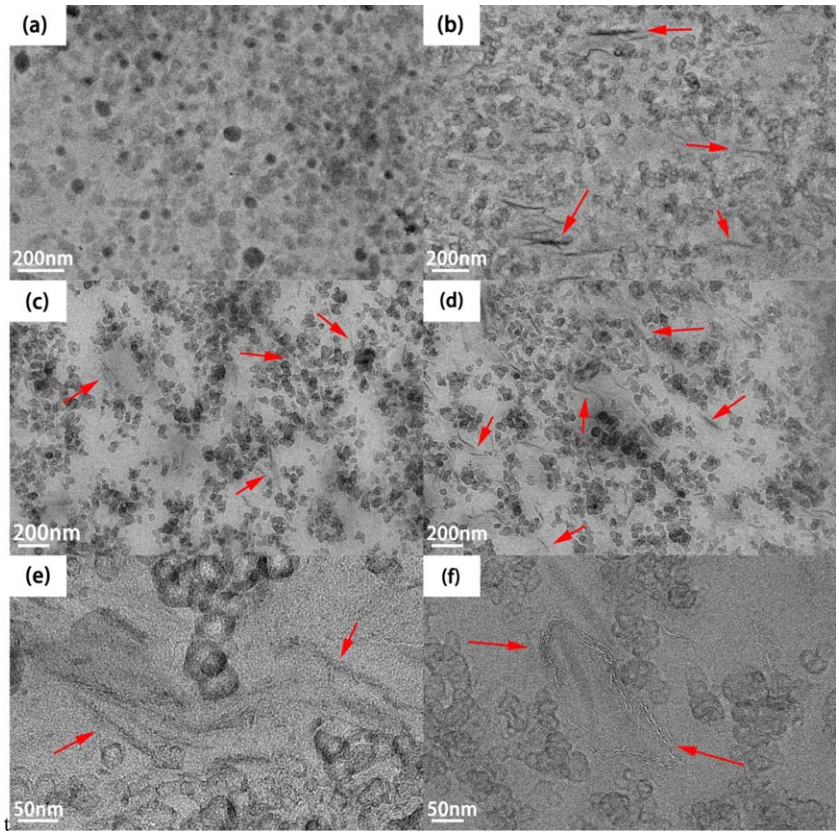

Figure 5. Effects of substitution on the dispersion of the fillers in rubber matrix evidenced by TEM. (a) NG-0; (b) and (e) NG-5; (c) NRG-1; (d) and (f) NRG-5. [Color figure can be viewed in the online issue, which is available at wileyonlinelibrary.com.]

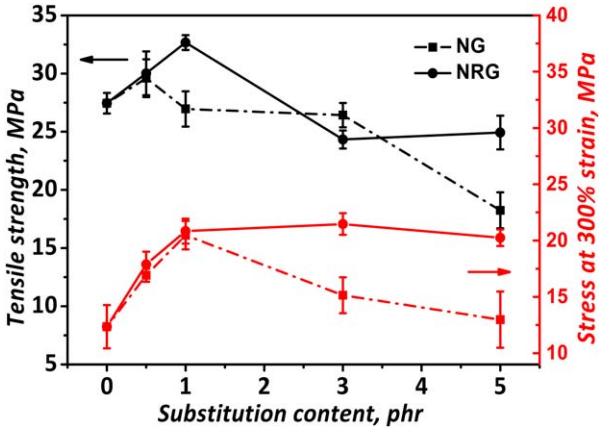

Figure 6. Effects of substitution on static mechanical properties of NR/CB composites. [Color figure can be viewed in the online issue, which is available at wileyonlinelibrary.com.]

dispersion of CB by the substitution of nanosheets in the composite may lead to improved static and dynamic mechanical properties of the composites.

Effects of the Substitution of GO or rGO on Static Mechanical Properties of NR/CB Composites

Figure 6 displays the static mechanical properties of NG and NRG composites. As shown in Figure 6, at lower substitution contents (not higher than 1 phr), the composites exhibit increased tensile strength, which is attributed to the high reinforcing capability of the nanosheets with high aspect ratio. The reinforcing effects of graphene-based materials have been ascribed to several factors including high aspect ratio, ultrastrong mechanical properties for graphene, interfacial stress transferring, facilitated stain-induced crystallization, improved dispersion of CB, and increased crosslink density.[7,29] However, as the nanosheets loading is further increased (higher than 3 phr), the tensile strength starts to decrease sharply, which may be due to the aggregation of GO or rGO sheets at higher concentration. Compared with GO, rGO exhibits better reinforcing effect, which is attributed to the better interfacial stress transferring in NRG.[7] Compared with the systems substituted by organo-modified layered silicate, the nanosheets we used here have shown higher reinforcement efficiency. In this study, when 1 phr of rGO is used, the tensile strength of composite increases by about 20%. However, Sapkota *et al.*[30] indicated that the incorporation of 1 phr of organo-clay did not change the tensile strength practically.

The dependences of modulus (stress at 300% strain) of composites on nanosheet content, as shown in Figure 6, are similar to the variation tendency of crosslink density. With substitution 1 phr GO or rGO for CB, the moduli of the both substituted composites increase by ~60% in comparison to the control sample. Such increase in modulus is mainly due to the more developed filler network structure with GO or rGO, which forms more trapped rubber so that the effective volume of fillers increases.[25,31] When the GO content is higher than 1 phr, the modulus starts to decrease. Such observation could be interpreted by the combination of filler aggregation, and insufficient surface adhesion which is resulted from poor compatibility between GO and NR. Therefore, the composites with higher GO content exhibit lowered modulus. As described above, the rGO modified with TPs owns a better interface when incorporated with NR rubber, and facilitates an improved dispersion of CB, so that the modulus does not decrease practically at higher sheet content.

Mooney-Rivlin equation[32] was used to further evaluate the reinforcing effect of the substitution and the elastomeric network of these composites. Mooney-Rivlin equation is expressed as follows:

$$\sigma^* = \frac{\sigma}{\left(\lambda - \lambda^{-2}\right)} = 2C_1 + 2C_2/\lambda \qquad (3)$$

where σ is tensile stress, λ is stretch ratio, and C_1, C_2 are constants and independent of λ.

Mooney-Rivlin plots of NG and NRG compostes are depicted in Figure 7(a,b). In the region of small extension ratio ($\lambda^{-1} > 0.8$), tensile strain increases as σ^* decreases. In such extension range, filler network structure of the composites is gradually broken down and resulted in rapid decline of σ^*,

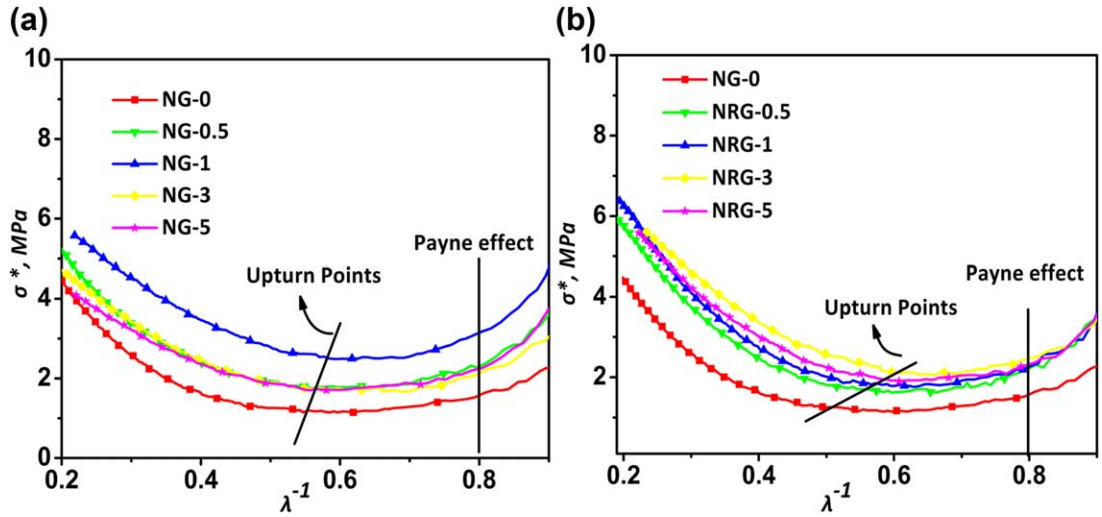

Figure 7. Mooney-Rivlin plots of NR/CB composites. [Color figure can be viewed in the online issue, which is available at wileyonlinelibrary.com.]

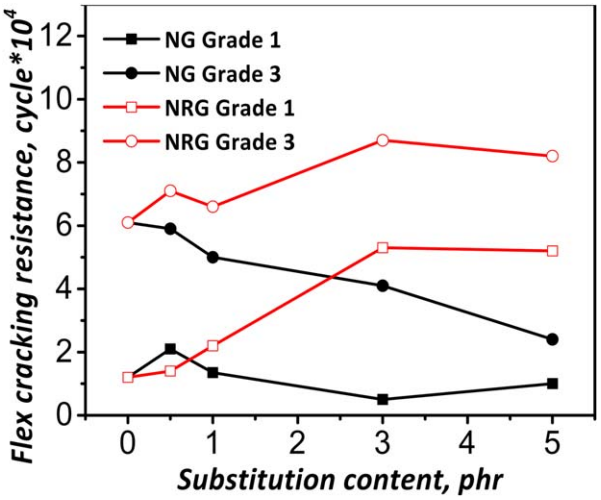

Figure 8. Effects of substitution on flex cracking resistance of NR/CB composites. [Color figure can be viewed in the online issue, which is available at wileyonlinelibrary.com.]

which can be attributed to Payne effect.[33] Later, with increasing tensile strain, $\sigma^*-\lambda^{-1}$ curves form a platform and have an abrupt upturn in the region of high extension ratio, which is primarily due to the uniform dispersion of high aspect ratio nanosheets giving rise to strain-induced crystallization of NR.[29,34] The upturn occurs as soon as the chains movement is limited by neighboring fillers. When the interactions between fillers and matrix become stronger, the chain mobility will be limited at a less strain and the upturn point will take place at smaller strain (higher λ^{-1}).[35] It can be concluded from the results that, as the mass fraction of nanosheets (both GO and rGO) substituted for CB increases, the value of λ^{-1} at the upturning point, increases firstly at lower substitution contents and then decreases gradually. NG composites achieve a peak value of λ^{-1} in NG-1 while NRG composites have one in NRG-3, which implies the strongest interaction between NR and hybrid fillers in each series.

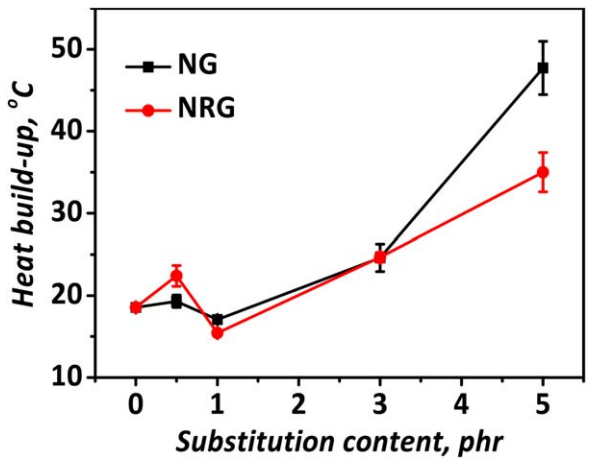

Figure 9. Effects of substitution on heat build-up of NR/CB composites. [Color figure can be viewed in the online issue, which is available at wileyonlinelibrary.com.]

Effects of the Substitution of GO or rGO on Dynamic Properties of NR/CB Composites

According to the GB/T 13934-2006 standard, the flex cracking resistance of vulcanizates is ranked into different levels, while Grade 1 means "needle-like points" (macroscopic number <=10) occur in the groove of samples, and Grade 3 means "needle-like points" extend to obvious cracks (one or more, and the length of crack is between 0.5 mm and 1.0 mm). As shown in Figure 8, addition of rGO improves the flex cracking resistance of NR/CB composites significantly, while GO deteriorates the cracking resistance. With 3 phr of rGO, the cycles of Grade 1 of flex cracking resistance are even tripled compared with the composite with CB only. It has been reported that graphene owns two competing effects on the flex cracking resistance of NR. At a lower strain, incorporation of graphene results in more cavities which will accelerate the crack growth. At a higher strain, graphene can retard the crack growth.[36] The pronounced improvement of flex cracking resistance may be attributed to the strain induced crystallization at a high flex strain, i.e., a higher crystallinity and a larger crystal zone are possibly achieved in NRG composites compared to that of NG-0.[36] The crack growth will be hindered by the formation of crystallites at the crack tip, and results in branch of crack, so more energy dissipation is allowed. It is worth noting that, when the amount of rGO increases to 5 phr, the flex cracking resistance of NR/CB composites is not improved and even declined, which is attributed to the aggregation of rGO in higher content and the formation of larger cavities near the crack tip. GO can hardly improve the flex cracking resistance of composites, on the contrary, the aggregation phenomenon of sheets will induce more stress concentrated points that sharply decrease the flex cracking resistance.

Heat build-up, measured with an elastomer cylinder under dynamic compression, is deemed to be the primary aging mechanism for rubber products in a dynamic loading environment. It is mainly determined by two aspects. One is the hysteresis of rubber matrix, and the other is the internal interactions of different networks, i.e., rubber−filler and filler−filler networks.[37] Generally the latter contribute more to heat build-up in most cases. Figure 9 shows that heat build-up of both two composites systems appears an overall increase with increasing substitution contents. As described above, the incorporation of the nanosheets leads to more developed filler network. As a result, the increase of substitution contents would enhance the internal frictions that increase the heat build-up of vulcanizates. With 5 phr of nanosheets substituting CB, heat build-up of NRG-5 is ~10°C lower than that of NG-5, which may be accounted to the better dispersion of CB and the more stable filler network compared to GO. As discussed in RPA results, filler network of NG is easier to be broken up than that of NRG under dynamic loading, which tend to increase the heat build-up because of more energy loss from "trapped rubbers" that are released when the filler networks are broken up.[25]

CONCLUSIONS

A latex mixing processing was used to disperse nanosheets including graphene oxide (GO) and reduced graphene oxide

(rGO) into natural rubber (NR), to study the effects of the substitution for carbon black (CB) with GO or rGO on the structure and performance of NR/CB rubber composites. Two series of NR/CB rubber composites with variable mass fraction of nanosheets (GO and rGO) were prepared. RPA results showed that the incorporation of the nanosheets led to formation of more developed filler network structure, while the one of rGO/CB appeared to be more stable than that of GO/CB as the strain increased. GO nanosheets retarded the curing process while rGO seems to have no detrimental effects on curing. Morphological observations substantiated better dispersion of CB when the nanosheets were incorporated. The improvements in static and dynamic mechanical properties were achieved. A small quantity of GO or rGO endowed the composites with a much higher modulus, and remarkable improvements in tensile strength. Besides, with substitution of rGO nanosheets, significant increase in flex cracking resistance was achieved, and NRG composites has a much lower heat build-up value compared to NG composites at a high loading of nanosheets. However, at a high concentration, both GO and rGO were apt to aggregate because of the strong interlayer forces among the nanosheets, which led to the poor efficiency on reinforcement and improvements in dynamic properties, and even causes damage to the performance of rubber composites.

ACKNOWLEDGMENTS

This work was supported by the National Natural Science Foundation of China (51222301, 50933001, and U1134005), the Research Fund for the Doctoral Program of Higher Education of China (20130172110001), and Fundamental Research Funds for the Central Universities (2014ZG0001).

REFERENCES

1. Mao, S.; Pu, H. H.; Chen, J. H. *RSC Adv.* **2012**, *2*, 2643.
2. Huang, X.; Qi, X.; Boey, F.; Zhang, H. *Chem. Soc. Rev.* **2012**, *41*, 666.
3. Hummers, W. S., Jr.; Offeman, R. E. *J. Am. Chem. Soc.* **1958**, *80*, 1339.
4. Stankovich, S.; Piner, R. D.; Nguyen, S. T.; Ruoff, R. S. *Carbon* **2006**, *44*, 3342.
5. Dreyer, D. R.; Park, S.; Bielawski, C. W.; Ruoff, R. S. *Chem. Soc. Rev.* **2010**, *39*, 228.
6. Stankovich, S.; Dikin, D. A.; Piner, R. D.; Kohlhaas, K. A.; Kleinhammes, A.; Jia, Y.; Wu, Y.; Nguyen, S. T.; Ruoff, R. S. *Carbon* **2007**, *45*, 1558.
7. Li, F. Y.; Yan, N.; Zhan, Y. H.; Fei, G. X.; Xia, H. S. *J. Appl. Polym. Sci.* **2013**, *129*, 2342.
8. Liao, R. J.; Tang, Z. H.; Lei, Y. D.; and Guo, B. C. *J. Phys. Chem. C* **2011**, *115*, 20740.
9. Zhao, X. Y.; Xiang, P.; Tian, M.; Fong, H.; Jin, R. G.; Zhang, L. Q. *Polymer* **2007**, *48*, 6056.
10. Rattanasom, N.; Saowapark, T.; Deeprasertkul, C. *Polym. Test.* **2007**, *26*, 369.
11. Du, M.; Guo, B.; Lei, Y.; Liu, M.; Jia, D. *Polymer* **2008**, *49*, 4871.
12. Chen, W. W.; Wu, S. W.; Lei, Y. D.; Liao, Z. F.; Guo, B. C.; Liang, X.; Jia, D. M. *Polymer* **2011**, *52*, 4387.
13. Kim, Y. A.; Hayashi, T.; Endo, M.; Gotoh, Y.; Wada, N.; Seiyama, J. *Scr. Mater.* **2006**, *54*, 31.
14. Dai, J. C.; Huang, J. T. *Appl. Clay Sci.* **1999**, *15*, 51.
15. Wang, M. J.; Mahmud, K.; Murphy, L. J.; Patterson, W. J. *Kautsch. Gummi Kunstst.* **1998**, *51*, 348.
16. Qu, L. L.; Huang, G. S.; Zhang, P.; Nie, Y. J.; Weng, G. S.; Wu, J. R. *Polym. Int.* **2010**, *59*, 1397.
17. Ma, P. C.; Liu, M. Y.; Zhang, H.; Wang, S. Q.; Wang, R.; Wang, K.; Wong, Y. K.; Tang, B. Z.; Hong, S. H.; Paik, K. W.; Kim, J. K. *ACS Appl. Mater. Inter.* **2009**, *1*, 1090.
18. Wang, Z.; Meng, X. Y.; Li, J. Z.; Du, X. H.; Li, S. Y.; Jiang, Z. W.; Tang, T. *J. Phys. Chem. C* **2009**, *113*, 8058.
19. Tang, Z. H.; Wei, Q. Y.; Lin, T. F.; Guo, B. C.; Jia, D. M. *RSC Adv.* **2013**, *3*, 17057.
20. Zhang, S. M.; Lin, L.; Deng, H.; Gao, X.; Bilotti, E.; Peijs, T.; Zhang, Q.; Fu, Q. *Express Polym. Lett.* **2012**, *6*, 159.
21. Galimberti, M.; Coombs, M.; Riccio, P.; Ricco, T.; Passera, S.; Pandini, S.; Conzatti, L.; Ravasio, A.; Tritto, I. *Macromol. Mater. Eng.* **2013**, *298*, 241.
22. Flory, P. J.; Rehner, J., Jr. *J. Chem. Phys.* **1943**, *11*, 521.
23. Flory, P. J. *J. Chem. Phys.* **1950**, *18*, 108.
24. Payne, A. R. *J. Appl. Polym. Sci.* **1962**, *6*, 57.
25. Wang, M. J. *Rubber Chem. Technol.* **1998**, *71*, 520.
26. Shanmugharaj, A. M.; Bae, J. H.; Lee, K. Y.; Noh, W. H.; Lee, S. H.; Ryu, S. H. *Compos. Sci. Technol.* **2007**, *67*, 1813.
27. Sepehri, A.; Razzaghi-Kashani, M.; Ghoreishy, M. *J. Appl. Polym. Sci.* **2012**, *125*, 204.
28. Quideau, S.; Feldman, K. S.; Appel, H. M. *J. Org. Chem.* **1995**, *60*, 4982.
29. Zhan, Y.; Wu, J.; Xia, H.; Yan, N.; Fei, G.; Yuan, G. *Macromol. Mater. Eng.* **2011**, *296*, 590.
30. Sapkota, J.; Poikelispää, M.; Das, A.; Dierkes, W.; Vuorinen, J. *Polym. Eng. Sci.* **2013**, *53*, 615.
31. Liu, Y. B.; Li, L.; Wang, Q. *J. Appl. Polym. Sci.* **2010**, *118*, 1111.
32. Rivlin, R. *Rubber Chem. Technol.* **1992**, *65*, 51.
33. Bokobza, L. *Macromol. Mater. Eng.* **2004**, *289*, 607.
34. Potts, J. R.; Shankar, O.; Du, L.; Ruoff, R. S. *Macromolecules* **2012**, *45*, 6045.
35. Tang, Z.; Wu, X.; Guo, B.; Zhang, L.; Jia, D. *J. Mater. Chem.* **2012**, *22*, 7492.
36. Yan, N.; Xia, H. S.; Zhan, Y. H.; Fei, G. X. *Macromol. Mater. Eng.* **2013**, *298*, 38.
37. Wang, Z. H.; Lu, Y. L.; Liu, J.; Dang, Z. M.; Zhang, L. Q.; Wang, W. M. *J. Appl. Polym. Sci.* **2011**, *119*, 1144.